International Journal of Environmental Studies

ISSN: 0020-7233 (Print) 1029-0400 (Online) Journal homepage: https://www.tandfonline.com/loi/genv20

A fast environmental change detection approach based on unsupervised multiscale texture clustering

Y. O. OUMA & R. TATEISHI

To cite this article: Y. O. OUMA & R. TATEISHI (2005) A fast environmental change detection approach based on unsupervised multiscale texture clustering, International Journal of Environmental Studies, 62:1, 79-93, DOI: 10.1080/0020723042000286374

To link to this article: https://doi.org/10.1080/0020723042000286374

Published online: 01 Feb 2010.

International Journal of Environmental Studies,
Vol. 62, No. 1, February 2005, 79–93

Routledge
Taylor & Francis Group

A fast environmental change detection approach based on unsupervised multiscale texture clustering

Y. O. OUMA*† AND R. TATEISHI‡

†Graduate School of Science and Technology, Chiba University, 1-33 Yayoi, Inage-ku, Chiba, 263-8522, Japan
‡Center for Environmental Remote Sensing, Chiba University, 1-33 YayoiInage-ku, Chiba, 263-8522, Japan

(Received in final form 10 August 2004)

In this paper, an analytic model for mapping land cover change that uses a novel multiresolution analysis in concert with image differencing to identify environmental change/no-change areas is presented. The method adaptively chooses thresholds to segment targets from background, by using multiscale decomposition of the image difference. Changes due to atmospheric influences are automatically suppressed and resolution heterogeneity problems minimized. Examples that demonstrate the efficiency of the technique on medium spatial resolution Landsat multitemporal imagery are presented. Empirical evaluation supports the suitability of this technique for fast identification of changed scenes. As opposed to the traditional change detection methods, we directly detect land cover changes rather than simply pixels. This is evident from the less-pixelated appearance of the change maps. The technique is recommended for regional/local environmental vulnerability and risk assessment as well for automated updating of GIS databases.

Keywords: Remote sensing; Automated environmental change detection; Wavelet transforms; Multiresolution analysis

1. Introduction

The natural environment is constantly placed under significant pressure arising from the increasing demands of economic and population growth. Management of the environment requires constant knowledge of the resulting changes and their effects on land-use/land-cover (LULC). However, the existence and/or extent of the LULC change cannot be adequately analyzed and understood using traditional methods and techniques in environmental science and physical geography.

Frequently used change detection methods can be divided into enhancement and post-classification techniques [1,2]. These methods have their own merits and demerits. For instance post-classification comparison provides direct information on nature of land cover

*Corresponding author. Email: yashon@graduate.chiba-u.jp

International Journal of Environmental Studies
ISSN 0020-7233 print: ISSN 1029-0400 online © 2005 Taylor & Francis Group Ltd
http://www.tandf.co.uk/journals
DOI: 10.1080/00207230420002863 74

changes, which are less dependent on the image coregistration and temporal normalization. However, they are often strongly dependent on the accuracy of the classifiers employed in the process. Enhancement techniques are often more accurate in the detection of areas exhibiting spectral change. However, the results may not necessarily be consistent with true land cover change, and they often need further analysis in order to extract information on the nature of the change. Enhancement techniques also require more accurate image coregistration and temporal normalization. One other problem with most of these procedures is that they are time consuming and rely heavily on human recognition, implying they are not reproducible.

The traditional techniques do not answer the following questions with regards to change detection and modeling for environmental monitoring and management in a timely and effective manner:

(1) has any change occurred – change/no-change detection within a timeframe;
(2) where has the change occurred – spatial extent of the change;
(3) what kind of change has occurred – categorization of change.

From remote sensing data, LULC change detection and analysis faces additional challenges, with regards to environmental change monitoring: (1) every imagery source has its own geometric, spatial, temporal and spectral characteristics; (2) noise is often visualized as change and is non-linear for every data; and (3) data amounts used in change detection are often voluminous. The problems and limitations associated with single-date land cover information extraction are compounded when attempting to produce land use change information using multitemporal data.

We can adequately conclude that automated production of spatially-detailed and thematically accurate land use and land cover information from satellite image data continues to be a challenge for the remote sensing research and application community.

Here, we propose an approach that tries to extract LULC change based on image transformation and multiresolution analysis as an unsupervised rapid LULC change detection technique. The proposed strategy determines changes via image differencing from the first principal component transformed (PCT) images. Resulting change images are decomposed using wavelet transform algorithm into different texture (spatial) scales. Temporal changes are detected while no-change is suppressed. We are able to effectively visualize the areas of change in the first, second and third scales from the Landsat ETM+ (2001), Landsat TM (1986) and Landsat MSS (1976) imagery. The results are promising for rapid change monitoring and as a strategy for environmental database updating processes.

2. Data preparation

2.1. Experimental data and study site

During the past 30 years, the Lake Nakuru basin has been transformed from sparsely populated and densely forested expanse into a region that is heavily settled, extensively cultivated and rapidly urbanizing. A key driver has been substantial increase in human population, resulting from both past and continuing high fertility and extensive in-migration.

The data used in this study and study site are presented in table 1 and figure 1, respectively. The geometric correction of the datasets was performed using image-to-image registration in

Table 1. Experimental data.

Test Site	Data	Size	Resolution (m)	Date of Acquisition
Lake Nakuru Basin	Landsat ETM+	1024 × 1024	30	3Apr2001
	Landsat TM	1024 × 1024	30	28Jan1986
	Landsat MSS	512 × 512	60	25Jan1976
	1: 50, 000 (TOPO) 1:250,000 (VEG)	1 Sheet #	–	1997 revised 1976 #

ENVI 3.6 Software. The reference image being the Landsat ETM+ since it has better geometric calibration than the other Landsat data.

As shown in Table 1, three different sensors are used in this study. The datasets have adverse fluctuations with respect to: spatial, temporal and spectral characterization resulting from differences in the sensors, acquisition and phenological differences.

3. Methodology

We begin our approach with the simplest theory of change detection via pixel-to-pixel subtraction, as opposed to the alternate popular method of first segmenting the two images

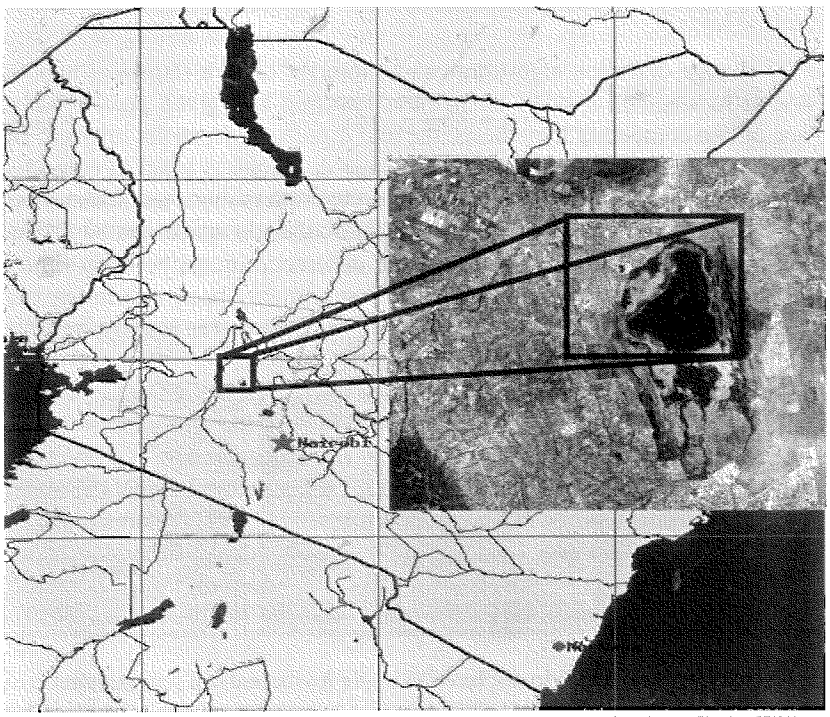

Figure 1. Location map of study site (Lake Nakuru Basin).

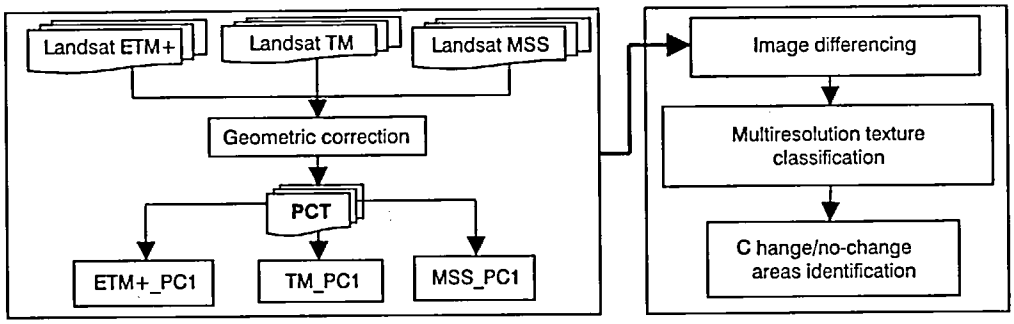

Figure 2. Conceptual framework for LULC change detection analytic model.

into regions and then comparing the derived objects to see what change has occurred. Since there are temporal differences between the input image sets, it can be expected that there will be intensity differences between the images, as well as some amount of misregistration. We first detect pixel-level differences and then build those differences into potential change areas automatically using multiresolution segmentation.

The general framework for our LULC change detection included first geometric correction, PCT, image differencing and finally texture based change extraction with wavelet transformation. Figure 2 presents the conceptual framework adopted in this research.

3.1. Theoretical basis

Almost every change detection algorithm can be thought of as a statistical hypothesis test. The decision as to whether or not a change has occurred at a given pixel x boils down to choosing one of two competing hypothesis: the *null hypothesis* H_0 or the *alternative hypothesis* H_1, corresponding to the *no-change* and *change* decisions at pixel x, respectively. The decision at pixel x generally involves evaluating a cost function (or test statistic) and selecting a suitable decision threshold. In many approaches, the test statistic is based on a simple difference image $[D = I_{t2} - I_{t1}]$. Where D is the difference image between time $t2$ and $t1$ images. Deriving changed areas from this result has arguably been a daunting task. In this study, we propose an alternative technique based on multiresolution analysis to determine the change/no-change areas.

One of the features that play an important role in the representation of landscape is terrain texture. It is also one of the most difficult features to describe and identify by a machine. Texture classification may be roughly divided into two categories: structural and statistical. Methods that can handle the more structured textures use structural models of texture, which assume that textures are composed of texture primitives. Statistical features based on second-order gray level statistics and gray level difference statistics have been studied extensively since the recognition [3], who proposed several features based on the co-ocurrence matrix. More recently, model-based approaches related to Markov Random Field (MRF) models, have been investigated [4,5].

In general, natural phenomena do not have a simple mathematical representation and do not even obey the restrictions imposed by several methods in order to be applicable. This fact has stimulated the search for new tools to describe variability of the landscape. In this direction, it

is worth mentioning fractal techniques [6], chaos theory and the rather new tool, here used, wavelet transform. This paper focuses upon the application of wavelet transform to the spatial image analysis and to assess landscape structure or variability for change features extraction.

3.2. Principal components transformation (PCT)

PCT was adopted to minimize the band redundancies and eliminate noise. This results in better discrimination of the actual temporal differences. The first PCT (PC1) images of the test data sets were chosen for the subsequent analysis since they contain the largest (>90% of the original image information) percentage of the total variance and have the maximum signal-to-noise ratio. PCT thus (1) excludes any outliers and (2) reduces redundancy due to high correlation in the Landsat images. Figures 3 and 4 show the false color composites and the associated first PCT images for MSS, TM and ETM+ respectively. The PCT results were scaled with mean brightness value of 127.5. This is termed here as intensity normalization or tonal balancing to take into account temporal and phenological differences. The histogram plots of the normalized PCT images are shown in figure 5.

3.3. Change detection

Image differencing is the simplest change detection approach. We let $I_{t1} : R^l \rightarrow R^k$ and $I_{t2} : R^l \rightarrow R^k$ be two images. That is, each image maps a pixel coordinate $x \in R^l$ to an intensity or color $I(x) \in R^k$. Typically, $k = 1$ (for gray-scale images) or $k = 3$ (for RGB color images), but other values are possible and $l = 2$ (e.g. satellite/surveillance imagery). Assuming that a typical change detection algorithm takes the images I_1 and I_2 as input and generates a binary image $B : R^l \rightarrow [0,1]$ called a change mask that identifies changed regions in the two images according to some generic rule for example:

$$B(X) = \begin{cases} 1 & \text{if pixel correspond to significant change from } I_1(x) \text{ to } I_2(x) \\ 0 & \text{otherwise} \end{cases}$$

Difference images generated by subtracting image values of one date from those of a corresponding layer from a second date highlight areas of changing land cover between two dates.

(a) (b) (c)

Figure 3. False color composites (FCC) of the test site for: (a) Landsat MSS 321-FCC; (b) TM 432-FCC; (c) ETM+ 432-FCC.

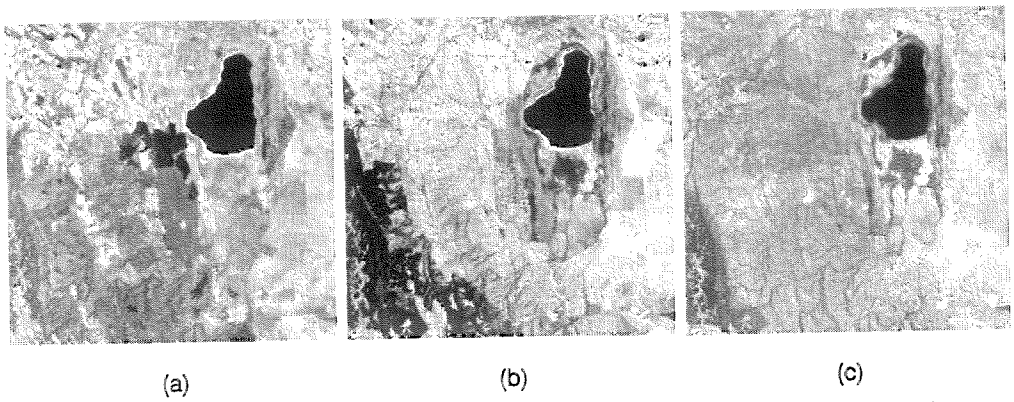

Figure 4. First principal component (PC1) images of: (a) Landsat MSS_PC1; (b) TM_PC1; (c) ETM+_PC1.

Difference images may be viewed a single layer at a time (gray-scale), or three difference image layers can be viewed together, one in each color plane. However, empirical determination of change/no-change (threshold) must be applied. This makes image differencing based decisions slow and biased for change quantification and/or qualification.

Figure 5 shows the change/no-change results of the difference images. It is not possible to automatically view the changes, not unless we apply a threshold based on some experience. This is often a time consuming and non-reproducible approach to change detection.

3.4. Texture classification

Image texture features contain information about the spatial distribution of image pixels. There are many methods for the computation and extraction of texture features including gray level statistics, laws masks, fourier transform, etc. The shortcoming of these methods is that they cannot analyze signals both in spatial and frequency domains simultaneously. Recent developments in spatial/frequency analysis such as the Gabor transform and Mallat wavelet transform provide good multiresolution analytical tools that should help in effective multiscale feature-texture analysis.

In §3.4.1 we briefly discuss the theory of scale-based decimated discrete wavelet transform (DDWT) as used in multiresolution analysis for change detection in two discrete time-intervals.

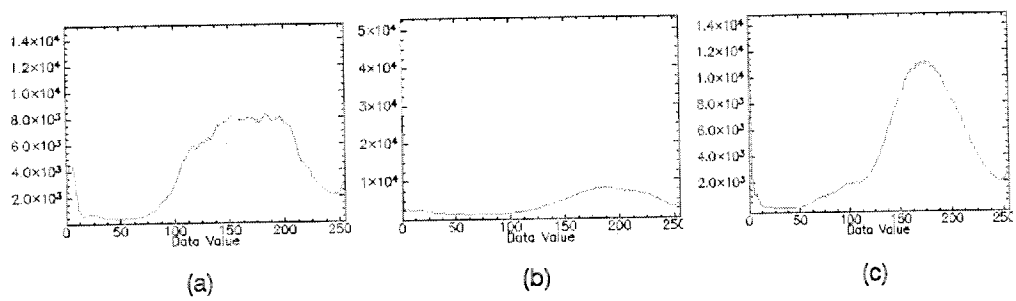

Figure 5. First PCT image histogram plots for: (a) MSS; (b) TM; (c) ETM+. The y-axes represent the frequency.

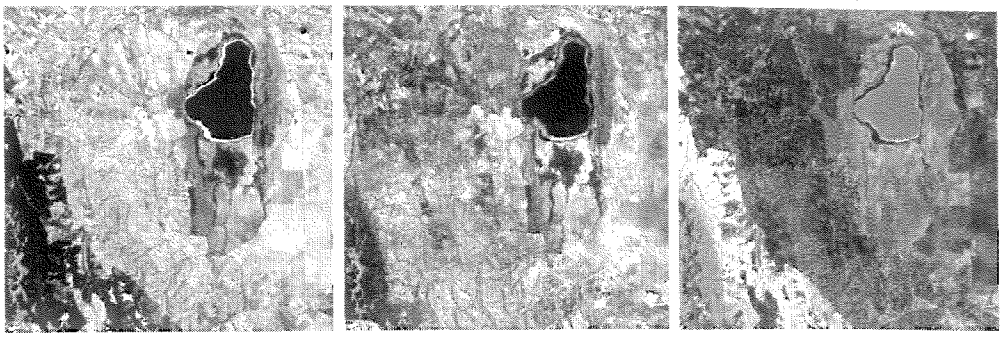

(a) (b) (c)

Figure 6. First principal component (PC1) difference – change images: (a) (TM_PC1)-(MSS_PC1); (b) (ETM+_PC1)-(MSS_PC1); (c) (ETM+_PC1)-(TM_PC1).

3.4.1. Multiresolution analysis (MRA) – Mallat 2-D discrete wavelet transform. The MRA provides a hierarchical pyramid for interpreting the image in terms of structures (details). After one resolution step in the decomposition process, the image containing the structure information for scales that are greater than the current scale is called context image, or smooth image. If the analysis is pursued, this context image will be in turn decomposed in details and another context image. In the discrete case, the details and the context images are obtained by filtering and sub-sampling of the original image.

The multiresolution wavelet transform decomposes a signal into coarser resolution representation, which consists of the low frequency approximation and high frequency detail information. Let the convolution of two energy finite functions, $F(x, y) \in L^2(R)$; where R is the real numbers and L^2 is the set of all functions, the approximation of a 2D finite energy function $f(x,y)$ at resolution 2^j, where integer j is a decomposition level, can be characterized by the coefficient calculated by the following convolution:

$$A_{2^j} f = ((f(x,y) \times \phi_{2^j}(-x)\phi_{2^j}(-y))(2^{-j}n, 2^{-j}m)_{(n,m)\in Z^2}$$

where m, n are integers; $\phi(x)$ is a 1D scaling function; and $\phi_{2^j}(x) = 2^j \phi(2^{-j}x)$. In general the $\phi(x)$ is a smoothing function whose Fourier transform is concentrated in low frequencies. The difference between approximation information at two consecutive resolutions 2^j and 2^{j-1}, which are characterized by $A_2^j f$ and $A_2^{j-1} f$, respectively, can be captured by the detail coefficients computed by the following convolutions:

$$D^1_{2^{j-1}} f = ((f(x,y) \times \phi_{2^{j-1}}(-x)\psi_{2^{j-1}}(-y))(2^{-(j-1)}n, 2^{-(j-1)}m)_{(n,m)\in Z^2}$$

$$D^2_{2^{j-1}} f = ((f(x,y) \times \psi_{2^{j-1}}(-x)\phi_{2^{j-1}}(-y))(2^{-(j-1)}n, 2^{-(j-1)}m)_{(n,m)\in Z^2}$$

$$D^3_{2^{j-1}} f = ((f(x,y) \times \psi_{2^{j-1}}(-x)\psi_{2^{j-1}}(-y))(2^{-(j-1)}n, 2^{-(j-1)}m)_{(n,m)\in Z^2}$$

where $\psi(x)$ is a 1D-wavelet function and $\psi_{2^j}(x) = 2^j \psi(2^j x)$. The wavelet function $\psi(x)$ is a band-pass filter. $A_{2^j} f$ can be perfectly reconstructed from $A_{2^{j-1}} f, D^1_{2^{j-1}} f, D^2_{2^{j-1}} f$ and $D^3_{2^{j-1}} f$, which are the context, vertical, horizontal and diagonal sub-images [7]. Figures 7 and 8 illustrates the multiresolution-based procedure.

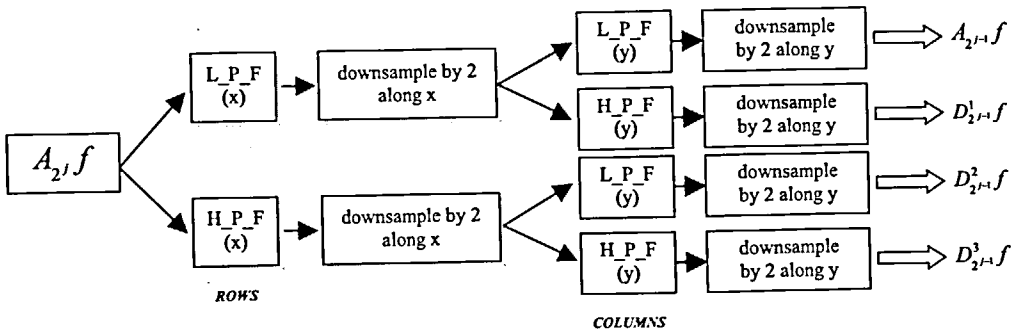

Figure 7. The decomposition of an image $A_{2^j}f$ into 4 sub-images.

The L_P_F is the scaling function representing the low frequency components, while H_P_F, which is the wavelet function, gives the high frequency components.

Mallat's [7] experiment suggests that by using wavelet decomposition, statistics based on first-order distribution of gray levels might be sufficient for preattentive perception textural difference. To obtain features that reflect scale-dependent properties, a gray-level feature is extracted from each scale separately and their texture energy assessed.

An appropriate quantity for analyzing object segmentation using this method is the texture energy expressed as:

$$E^i_j = \frac{1}{MN}\sum_{m=1}^{M}\sum_{n=1}^{N}(D^i_j(m,n))^2$$

where M, N = the size of given scope; $D^i_j(m,n)$ = the element of sub-images from wavelet transform; j = the direction of the wavelet transform and i = the depth of wavelet transform. These wavelet energy signatures E^i_j reflect the distribution of energy along the frequency axis over scale and orientation, which may vary according specific feature characteristics.

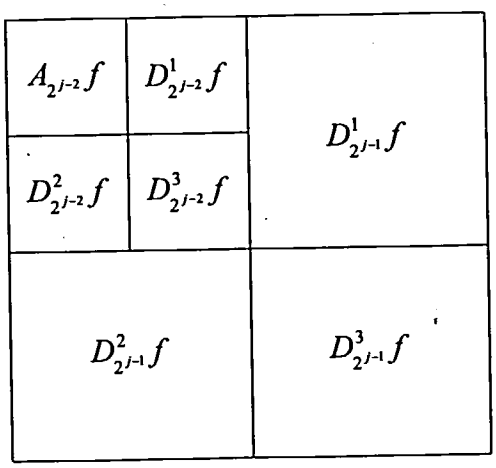

Figure 8. Example wavelet representation pyramid structure.

Wavelet transform has a number of advantages over other transformation and multiresolution analysis methods. One is spatial discrimination and second is multiscale representation. These advantages make it more adaptable to scale-based-object change detection.

4. Results and discussion

By applying the wavelet decomposition, we determine the change from no-change areas automatically from the difference imagery, as explained in §4.2. The potential of the proposed change detection scheme is demonstrated by analyzing different feature-regions of the land cover types.

4.1. Object change segmentation using wavelet

Since the datasets have been acquired over large and diverse geographic regions characterized by three different Landsat sensors, true land cover changes due to, for example, deforestation and loss of vegetation are often complicated by other coexisting adverse fluctuations. These adverse fluctuations do not represent true land cover changes as explained in §2.1. We argue that through resolution decomposition, it is possible to derive explicitly the changes from insignificant changes.

Figures 9–11 show the level 1 results of the change decomposition sub-images in the vertical, horizontal and diagonal features, using Mallat's discrete 2D-wavelet transform. At individual levels it is not obvious where there is change or no-change through independent analysis.

Figure 12 shows the binary encoded histogram evaluation of the change pixels in the gray-image (figure 6(a)) and in the wavelet-sub-images. The different peaks represent the change pixels for different change land cover, which also correspond to the feature texture energy.

In order to extract the changed areas, we apply a high pass filter since the change information is associated with the high frequency-signal component of the image as illustrated in figure 12 above. Figure 13 shows the change extraction processing flow. The suggested clustering can be carried out with any unsupervised classification algorithm.

In order to analyze the classes further we constrain our analysis to allowable changes only as shown in table 2.

(a) (b) (c)

Figure 9. (TM-MSS) level 1 change sub-image: (a) vertical; (b) horizontal; (c) diagonal features.

(a) (b) (c)

Figure 10. (ETM+-MSS) level 1 change sub-image: (a) vertical; (b) horizontal; (c) diagonal features.

4.2. Change detection and analysis

In this section, we present results for changes between 1976–1986 and 1986–2001. To evaluate some of the results of this research, we take a case of an expanding urban area (blue rectangle) for illustration. Figures 14 and 15 show snapshots of these features/areas in the 432 false color composite.

The red triangle indicates the urban change from 1976 to 1986. This is the same scene as figure 14. At level 1, the blue reflecting pixels represent changes associated with urban land use. These are mostly residential/concrete surfaces. Level 2 shows changes mostly associated with vegetation, as green. Thus interpretation of the results of both levels is essential for understanding the different levels of change. The rest of the levels do not show significant information, due to the coarse spatial resolution. At each level, different spectral clusters represent different class conversations while the 0-gray values represent no changes.

In Figures 16 and 17, we present the false color composites of change/no-change between (TM and MSS), and (ETM+ and TM) respectively. Due to the immense amount of change between (1976–2001), we do not present the results here. Most of the change areas are in blue and these are mostly urbanization and agricultural activities.

(a) (b) (c)

Figure 11. (ETM+-TM) level 1 change sub-image: (a) vertical; (b) horizontal; (c) diagonal features.

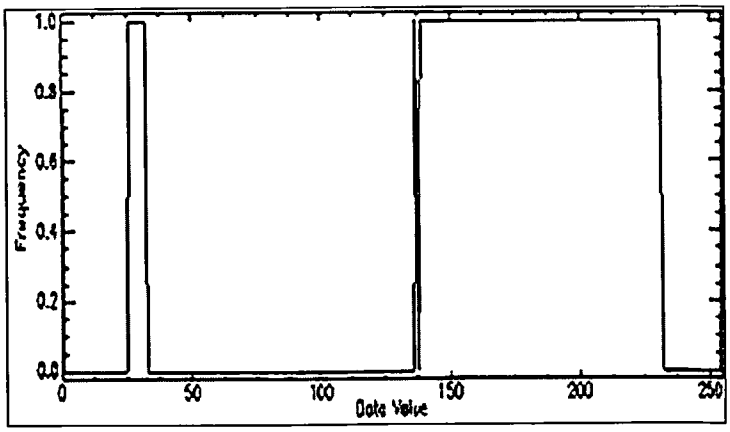

(a)

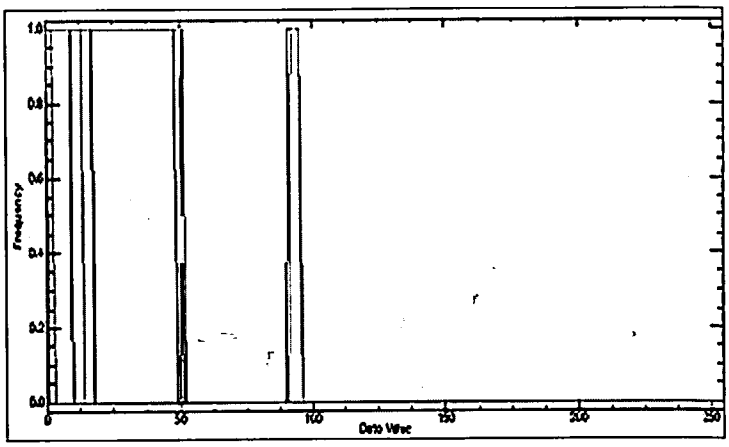

(b)

Figure 12. Change pixel histogram distribution in: (a) gray-image; (b) and wavelet sub-bands. The peaks in the gray-scale image are split in the wave-let sub-bands.

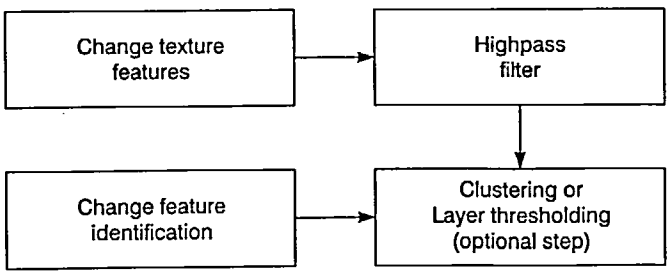

Figure 13. Change/no-change map generation. This phase separates the high frequency information.

Table 2. Allowable change and no-change land cover combinations. (–) implies no change, else possible change.

From→To	Urban	Vegetation	Agriculture	Forest	Bare
Urban				–	
Vegetation					
Agriculture				–	–
Forest	–				–
Bare			–	–	

It is imperative to mention that it is nearly impossible with methods like image-differencing, post-classification comparison to accurately identify change pixels based. This is as a result of not only the radiometric and spatial differences but also it may be too complex to derive an accurate the change decision.

Between 1986–2001, the results are shown in figure 17. Figure 17(a) shows the same urban area as that depicted in figure 16. Again the blue pixels represent changed urban pixels. Other changes within the urban area are represented with different tones. In figure 17(b), major changes in part of Nakuru Town are shown with blue pixels. The white reflecting pixels within the white square are changes due to the construction of sewer plant. In figure 17(c), mostly vegetation changes appearing as green pixels are shown especially around the lake and within the town. While green represents more vegetation, pink are areas where vegetation has been replaced for urban development.

5. Conclusion

The dynamism of LULC is complex and it is suggested that it can best be understood through hierarchical spatial-scale analysis. With the vast amount of remote sensing data, techniques involving human recognition are not robust enough for fast multitemporal change analysis. Through spatial-scale analysis, it is demonstrated that it is possible to discriminate change

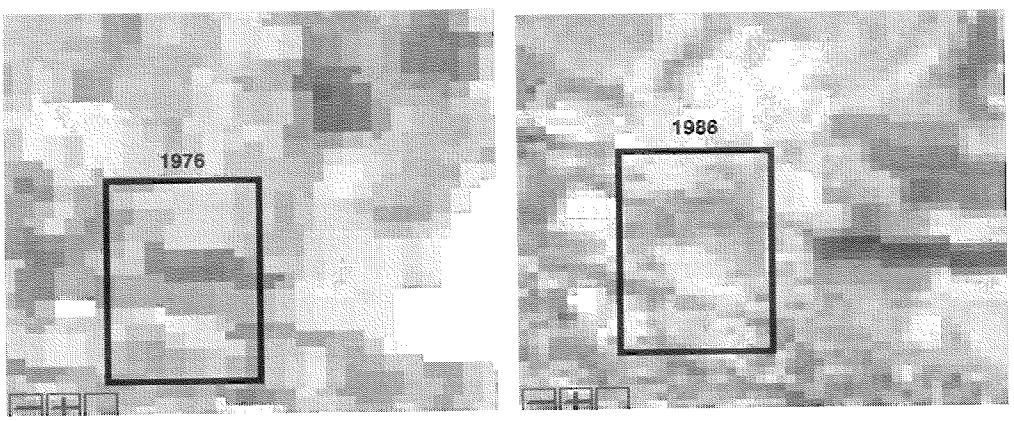

Figure 14. Urban agglomeration between 1976–1986 test scene within rectangle.

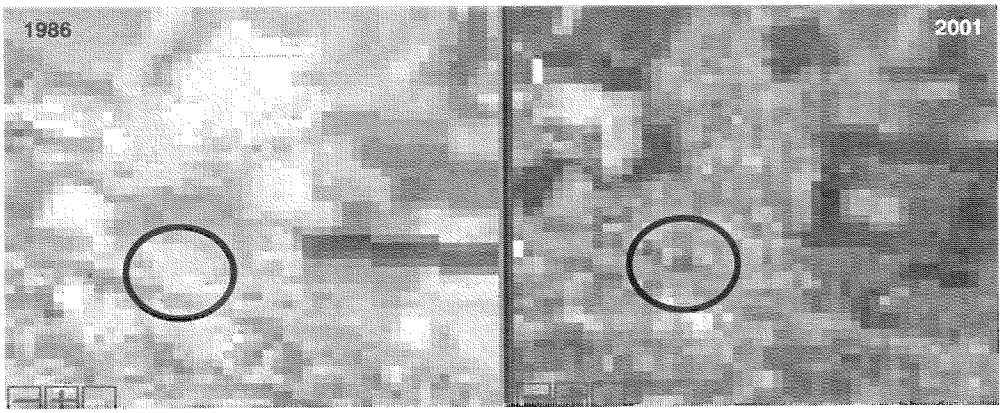

Figure 15. Urban agglomeration between 1986–2001 (snapshot). The circles indicate one of main urbanization change areas.

from no-change. With this approach, we are able to quickly pinpoint the main change areas. Even though the changes are well discriminated, their quantification is not accurately possible at the resolutions of the resulting scales.

5.1. Testing different wavelets

It was found that with wavelets that are not symmetric such as Daubechies, Symlet, Coiflet, some biorthogonal spline family wavelets may not be suitable for object/feature extraction. Given that in our case feature positions are very necessary, these types of wavelets shift the positions of features/objects, which makes further comparison impossible. Also, for these other wavelets, during the decomposition, it is observed that the scaling function forces the

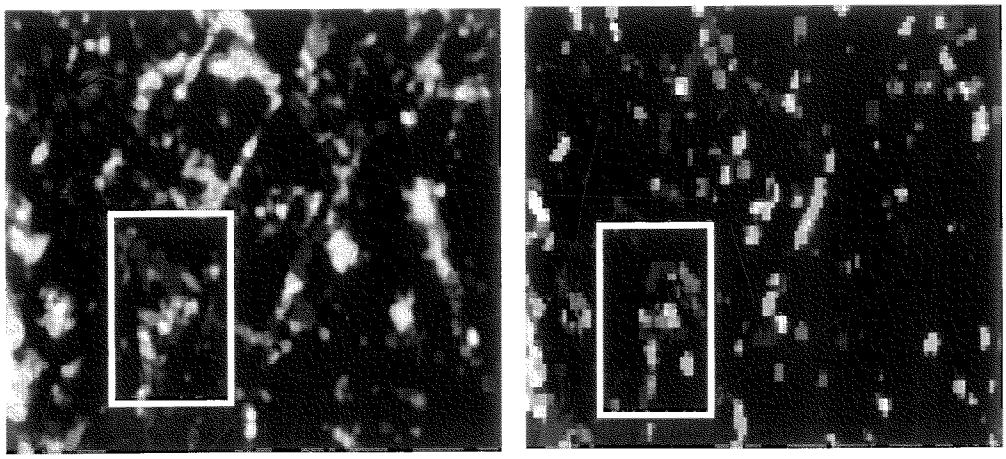

Figure 16. [TM-MSS] change/no-change at: (a) level 1; (b) level 2. Most of the blue pixels are urban converted changes.

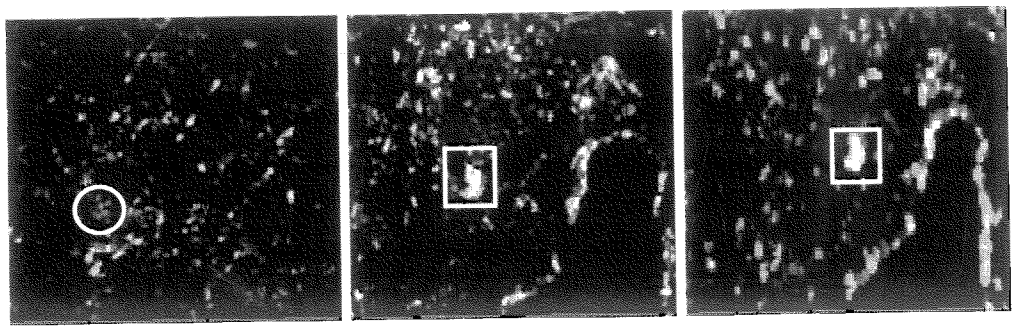

(a) (b) (c)

Figure 17. Wavelet transform composites for (1986–2001): (a) level 1 showing the same urban area; (b) level 1showing the main changes in Nakuru town and the environs; (c) level 2 results of the same site as (b). The square shows the sewer plant (white reflecting pixels) location change.

approximation data to comply with its waveform. This implies that at large scales, the approximation is highly distorted by scaling function. Mallat wavelet is thus considered the most suitable for this task.

5.2. Land cover change detection and analysis

The test results are influenced by the complexity and spatial resolution of objects. It is worth noting that the test area was selected to represent the most difficult situation. Although the results do not separate the change objects explicitly, the strategy used in this research would be more feasible with higher spatial resolutions, e.g. ≤15 m.

Conventional methods for change detection, such as image-differencing alone, multidate principal components transformation, multidate clustering or RGB-NDVI color composite change detection, obviate the need for a high degree of *a priori* knowledge, but require substantial *a posteriori* interpretation. The method addressed in this research explicitly identify *a priori* and *a posteriori* the types and natures of land cover changes within the multitemporal remote sensing data. Our approach is a prototypical change detection system that: (1) minimizes elaborate human recognition in the change detection process; (2) minimizes noise from change detection process; and (3) automatically detects change/no-change regions emphasizing different land cover at different resolutions or scales. We also argue that as opposed to the traditional change detection, we are dealing with objects directly rather than simply pixels. This is evident from the less-pixelated appearance of the change maps.

Some of the contributions to which this research can be extended include: rapid environmental change priority and vulnerable zones identification, and automated GIS database upgrading by selecting changed areas. Changed areas are rapidly identified by direct composite display avoiding any threshold definitions.

This study demonstrates the fact that land cover changes are dependent on the spatial and temporal domains at which they are assessed. Shorter temporal domains with better spatial resolutions are envisaged to yield better results. Our future research is to adopt a change componentization system that implicitly extracts changes with respect to spatial and spectral characteristics resulting from multiscale analysis.

References

[1] Pilon, G.G., Howarth, P.J., Bullock, R.A. and Adeniyi, P.O., 1988, An enhanced classification approach to change detection in semi-arid environments. *Photogrammetric Engineering and Remote Sensing,* **54**(12), 1709–1716.

[2] Singh, A., 1989, Digital change detection techniques using remotely-sensed data. *International Journal of Remote Sensing,* **10**(6), 989–1003.

[3] Haralick, R.M., Shanmugam, K. and Dinstein, I., 1973, Textural features for image classification. *IEEE Trans on Systems, Man and* Cybernetics, **SMC-3**(6), 610–621.

[4] Leguizamón, S., 1992, Description of terrain textures by fractal and markov random fields techniques. *Proc. of the 2nd Int. Symposium on High-Mountain Remote Sensing Cartography,* Beijing & Lhasa, PR China,. pp. 91–99.

[5] Derin, H. and Elliot, H., 1987, Modeling and segmentation of noisy and textured images using Gibbs random fields. *IEEE Trans. on Pattern Analysis and Machine Intelligence,* **vol. PAMI-9,** 39–55.

[6] Mandelbrot, B.B., 1982, *The Fractal Geometry of Nature* (San Francisco, CA: Freeman).

[7] Mallat, S.G., 1989, A theory for multiresolution signal decomposition: the wavelet representation. *IEEE Transactions on Pattern Analysis and Machine Intelligence,* **12**(7), 629–639.